Relationship of Deregulated Signaling Converging onto mTOR with Prognosis and Classification of Lung Adenocarcinoma Shown by Two Independent *In silico* Analyses

Hiromichi Ebi,[1] Shuta Tomida,[1] Toshiyuki Takeuchi,[3] Chinatsu Arima,[1] Takahiko Sato,[1] Tetsuya Mitsudomi,[4] Yasushi Yatabe,[5] Hirotaka Osada,[2,6] and Takashi Takahashi[1]

[1]Division of Molecular Carcinogenesis, Center for Neurological Diseases and Cancer and [2]Department of Cellular Oncology, Nagoya University Graduate School of Medicine; [3]Division of Research and Development, Oncomics Co., Ltd.; Departments of [4]Thoracic Surgery and [5]Pathology and Molecular Diagnostics, Aichi Cancer Center Hospital; and [6]Division of Molecular Oncology, Aichi Cancer Center Research Institute, Nagoya, Japan

Abstract

There is marked disparity with a slight overlap among prognosis-predictive signatures reported thus far for lung cancers. In this study, we aimed at linking poor prognosis with particular pathways and/or functions of the gene sets involved to better understand the underlying molecular characteristics associated with the prognosis of lung adenocarcinomas. Gene set enrichment analysis identified a gene set down-regulated by rapamycin as the most significant, whereas several others responsive to withdrawal of glucose or amino acids, which are related to signaling converging onto mammalian target of rapamycin (mTOR), were also shown to be significantly associated, in addition to those related to DNA damage response and cell cycle progression. We also used connectivity map (C-MAP) analysis, an independent bioinformatics approach, to search for Food and Drug Administration–approved drugs that potentially transform an unfavorable signature to a favorable one. Those results identified inhibitors of phosphatidylinositol 3-kinase (PI3K) and mTOR, as well as unexpected drugs such as phenothiazine antipsychotics and resveratrol as potential candidates. Experimental validation revealed that the latter unexpected agents also inhibited signaling converging onto mTOR and exhibited antitumor activities. In addition, deregulation of multiple signaling converging onto mTOR was shown to be significantly associated with sensitivity to PI-103, a dual specificity PI3K/mTOR inhibitor that is not contained in the C-MAP database, lending further support for the connection. Our results clearly show the existence of gene set–definable, intrinsic heterogeneities in lung adenocarcinomas, which seem to be related to both clinical behavior and sensitivity to agents affecting the identified pathways. [Cancer Res 2009;69(9):4027–35]

Introduction

Adenocarcinomas exhibit the highest degree of morphologic and clinical diversities among the various types of lung cancers, and it is well recognized that their current pathologic classification and ability to predict postsurgical prognosis are quite inadequate. Although the existence of marked heterogeneity, including their expression profiles, is well appreciated (1), virtually all adenocarcinomas are currently treated similarly under the diagnosis of non–small cell lung cancer. Along this line, better understanding of molecular heterogeneities is considered to be one of the major factors that has significantly improved cure rates of certain types of neoplasia, such as hematologic malignancies and breast cancer. Thus, a better understanding of the underlying molecular mechanisms of the heterogeneities among lung adenocarcinomas is greatly anticipated to contribute to reducing the unbearably large number of deaths by establishing a foundation for rational individualized treatment strategies, as well as development of novel therapeutic methods.

The tumor-node metastasis staging system is currently used as the standard method for predicting prognosis, whereas a number of individualized molecular signature-based predictions that partition patients into distinct prognostic groups have also been developed, including our own, which have shown good results for predicting patients with dismal prognosis (2–6). However, there is a marked discordance with a slight overlap among such predictive signatures thus far reported for lung cancers. This disparity makes it difficult to reconcile them in relation to the underlying molecular characteristics, which has led to criticism stating that such models do not provide biological insight.

In this study, we used two independent bioinformatics approaches, gene set enrichment analysis (GSEA; ref. 7) and connectivity map (C-MAP; ref. 8) analysis, in combination with biological and biochemical experiments for validation, to elucidate the underlying molecular basis for the link of poor prognosis with particular pathways and/or functions of the gene sets involved. Consequently, well-defined and easily interpretable gene sets were identified as associated with fatal outcome, providing insight into the existence of intrinsic heterogeneities in lung adenocarcinomas and the usability of *in silico* screening for potential antitumor agents with activities to revert a fatal signature to a favorable one.

Materials and Methods

Bioinformatics and biostatistics analyses. Clinical characteristics, such as length of the follow-up period, are described in Supplementary Materials and Methods. The Nagoya data set of microarray analysis (GEO GSE 11969), previously reported by our group (1), was used in two independent bioinformatics analyses. Two additional data sets reported by Harvard (9) and Memorial Sloan-Kettering Cancer Center (10) groups were

Note: Supplementary data for this article are available at Cancer Research Online (http://cancerres.aacrjournals.org/).

H. Ebi and S. Tomida contributed equally to this work.

Requests for reprints: Takashi Takahashi, Division of Molecular Carcinogenesis, Center for Neurological Diseases and Cancer, Nagoya University Graduate School of Medicine, Showa-ku, Nagoya 466-8550, Japan. Phone: 81-52-744-2454; Fax: 81-52-744-2457; E-mail: tak@med.nagoya-u.ac.jp.

doi:10.1158/0008-5472.CAN-08-3403

also used for validation. GSEA was performed using the GSEA version 1.0 program for *R* (7). C-MAP analysis was performed using the tool[7] described by Lamb and colleagues (8). Detailed methodologic information for the present GSEA and C-MAP analyses is provided in Supplementary Materials and Methods. The CLUSTER program was used for average linkage hierarchical clustering of both genes and cases, whereas the TREEVIEW program was used for display (11). Fisher's exact test was performed to examine associations of the deregulation score–based clusters with various clinical parameters, whereas Cox regression analysis was used to analyze the relationships among various parameters, including deregulation score–based clusters and postoperative prognosis. All statistical tests were two sided.

Cell lines. ACC-LC-94, ACC-LC-176, and ACC-LC-319 cells were established in our laboratory, whereas the A549, A427, and NCI-H23 cell lines were purchased from the American Type Culture Collection. The SK-LU-1, SK-LC-3, SK-LC-5, and SK-LC-7 cell lines were generously provided by Lloyd J. Old (Memorial Sloan-Kettering Cancer Center). Cells were cultured in RPMI 1640 supplemented with 5% fetal bovine serum (Invitrogen-Life Technologies, Inc.).

Growth inhibition assays. Growth inhibition was assessed by an MTS assay using the TetraColor ONE kit (Seikagaku) according to the manufacturer's instructions. Each combination of cell line and drug was set up in six replicate wells, and the experiment was repeated at least thrice. Each data point presented in the assay results represents the growth of treated cells compared with untreated cells.

Small interfering RNA knockdown. A synthetic small interfering RNA (siRNA) duplex composed of rictor (Dharmacon) and scramble (QIAGEN) was transfected using Lipofectamine RNAiMAX (Invitrogen) according to the manufacturer's instructions. Twenty-four hours after siRNA transfection, cells were seeded (3×10^3/100 μL) into 96-well plates, incubated overnight, and treated with or without rapamycin for 72 h. Viability was measured using a 3-(4,5-dimethylthiazol-2-yl)-2,5-diphenyltetrazolium bromide (MTT) assay. Down-regulation of rictor was confirmed 5 d after transfection by Western blot analysis.

Results

Identification of gene sets associated with relapse in lung adenocarcinomas. We performed GSEA using our previous data set containing 90 lung adenocarcinomas (the Nagoya data set; ref. 1) to identify gene sets with a clear association with relapse. First, data from 42 favorable samples (alive >5 years after surgery without any evidence of relapse) and 33 fatal samples (dead with evidence of relapse after initial surgery) were extracted, and GSEA consequently identified eight gene sets with significant associations with a fatal outcome (Fig. 1*A* and *B*; Supplementary Tables S1–S5). A GSEA gene set, which was originally selected because of down-regulation in the presence of rapamycin (Rap_down), exhibited the most significant enrichment of all queried genes associated with relapse-related death. Three other significantly enriched gene sets included those reduced by either glucose deprivation (Glucose_down), leucine deprivation (Leu_down), or glutamine deprivation (Glut_down; Fig. 1*B*), which seemed to be consistent with the notion that the mammalian target of rapamycin (mTOR) is a converging point of growth factor receptor signaling with nutrient availability and energy status of the cell (12–14). For the sake of convenience, these gene sets are herein termed metabolic pathway gene sets. In addition, gene sets related to cell cycle and DNA damage signaling also showed a significant association with fatal outcome.

[7] http://www.broad.mit.edu/cmap/

Next, we determined whether similar gene sets could be selected by GSEA using the completely independent data set of 62 lung adenocarcinoma cases presented by the Harvard group, for which information regarding both relapse and death are available (9). The Leu_down ($P = 0.0238$), Cell_Cycle ($P = 0.0444$), and DNA damage signaling ($P = 0.0500$) gene sets were shown to be significantly associated with relapse-related death in that data set, whereas Rap_down ($P = 0.0833$), CR_cell_cycle ($P = 0.0851$), and Glut_down ($P = 0.0976$) were also included in the top 10 gene sets, although the results for those did not reach statistical significance. These findings further supported the involvement of these gene sets in signatures associated with clinical behavior (Supplementary Table S6).

Associations of deregulation of GSEA-identified gene sets with various clinicopathologic characteristics. To investigate associations between the levels of perturbation in each of the GSEA-identified gene sets and various clinicopathologic characteristics, we defined a "deregulation index" for each gene set, which was calculated by averaging the normalized gene expression values. The deregulation index values clearly separated between fatal and favorable prognosis (Fig. 1*C*; Supplementary Fig. S1), as well as between terminal respiratory unit (TRU) and non-TRU types, our previously proposed expression profile-substantiated classification of adenocarcinomas (Supplementary Fig. S2; ref. 1). Interestingly, even tumors from patients with a favorable prognosis exhibited a more prominent perturbation state than normal lung tissue samples. Hierarchical clustering analysis using the deregulation indices of the four metabolic pathway gene sets was also performed, which resulted in clear separation of two major branches (Fig. 2*A*). The right branch preferentially consisted of tumors with pronounced deregulation and characteristically harbored male gender and positive smoking history (Supplementary Table S7; $P = 0.019$ and $P = 0.002$, respectively). We also noted a significant association of deregulation state with the presence of bronchioloalveolar carcinoma features ($P = 0.002$), as well as with TRU type ($P < 0.001$; Supplementary Table S7). Mutations in the epidermal growth factor receptor (*EGFR*) and *K-ras* genes did not show any associations ($P = 0.659$ for *EGFR* and $P = 0.735$ for *K-ras*), although there was a tendency for a more prevalent presence of *p53* mutations in the right branch with greater deregulation ($P = 0.071$ for *p53*). Kaplan-Meier survival curves showed a significant difference in relapse-free survival between the high-deregulation and low-deregulation clusters, whereas multivariate Cox regression analysis revealed that deregulation cluster discrimination was a significant independent prognostic factor ($P = 0.009$) in addition to disease stage ($P = 0.009$; Fig. 2*B*).

The associations of deregulation state with prognosis and other variables were further validated using another independent data set from the Memorial Sloan-Kettering Cancer Center (10). Hierarchical clustering analysis based on the deregulation indices of the four metabolic pathway gene sets resulted in clear separation of two major branches, which showed that cases in the cluster with pronounced deregulation characteristically harbored positive smoking history ($P = 0.010$; Supplementary Table S8; Fig. 2*C*). Notably, we confirmed that cases with pronounced deregulation had significantly worse prognosis than those in the other cluster (Fig. 2*D*), whereas multivariate Cox regression analysis revealed that deregulation cluster discrimination was significantly associated with postoperative prognosis independent of disease stage ($P = 0.012$), further supporting the notion that deregulation of the metabolic pathways was a generic signature observed in patients with a high risk for relapse and fatal prognosis.

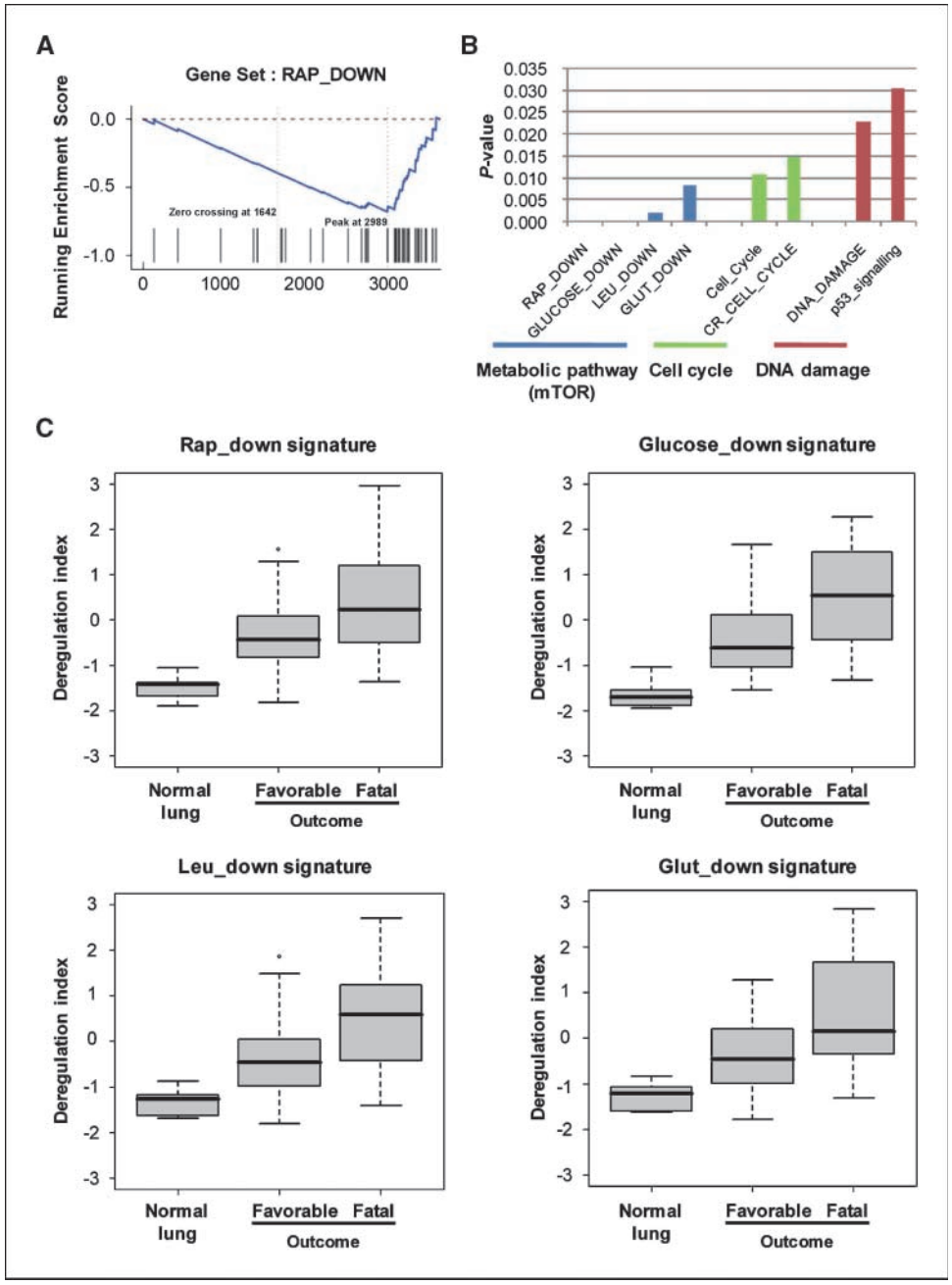

Figure 1. *A,* representative GSEA results showing significant enrichment of the Rap_down gene set in association with fatal outcome. *B,* list of gene sets in the Nagoya data set significantly associated with relapse-related death (nominal *P* values of <0.05). *C,* box plots showing a deregulation index for each metabolic gene set.

Search for Food and Drug Administration–approved drugs with potential to revert fatal signatures of the gene sets. To identify agents with antitumor effects by searching for those that potentially alter a fatal prognosis–associated signature to a favorable prognosis–associated one, we performed C-MAP analysis, another completely distinct bioinformatics method. C-MAP is a library of signatures of drug response in a database used for queries regarding expression information to clarify potential association with other biological contexts, thereby linking otherwise unrelated physiologic events (8, 15). For this analysis, we selected 477 probes derived from 332 up-regulated and 145 down-regulated genes that were significantly differentially expressed ($P < 0.05$ by t test) between those who survived without relapse for >5 years and those who died with relapse in 75 cases of lung adenocarcinomas in the Nagoya data set and used them as query items to compare to rank-ordered lists for each drug treatment in the C-MAP database. We identified multiple Food and Drug Administration (FDA)–approved drugs with a significantly biased appearance of the query genes closer to the top of the rank-ordered list, indicating the induction of significant down-regulation in 332 genes with relapse-related death-associated up-regulation by a given drug treatment, as well as significant up-regulation of the 145 genes down-regulated by the treatment (Table 1). The results of Kolmogorov-Smirnov scanning of the sixth-ranked sirolimus in the C-MAP analysis are shown in Fig. 3*A*, which showed enrichment of the favorable (down-regulated) and fatal (up-regulated) signatures, whereas summaries of all instances of sirolimus and LY-294002 are shown in Fig. 3*B*. Wortmannin and LY-294002, inhibitors of phosphoinositide

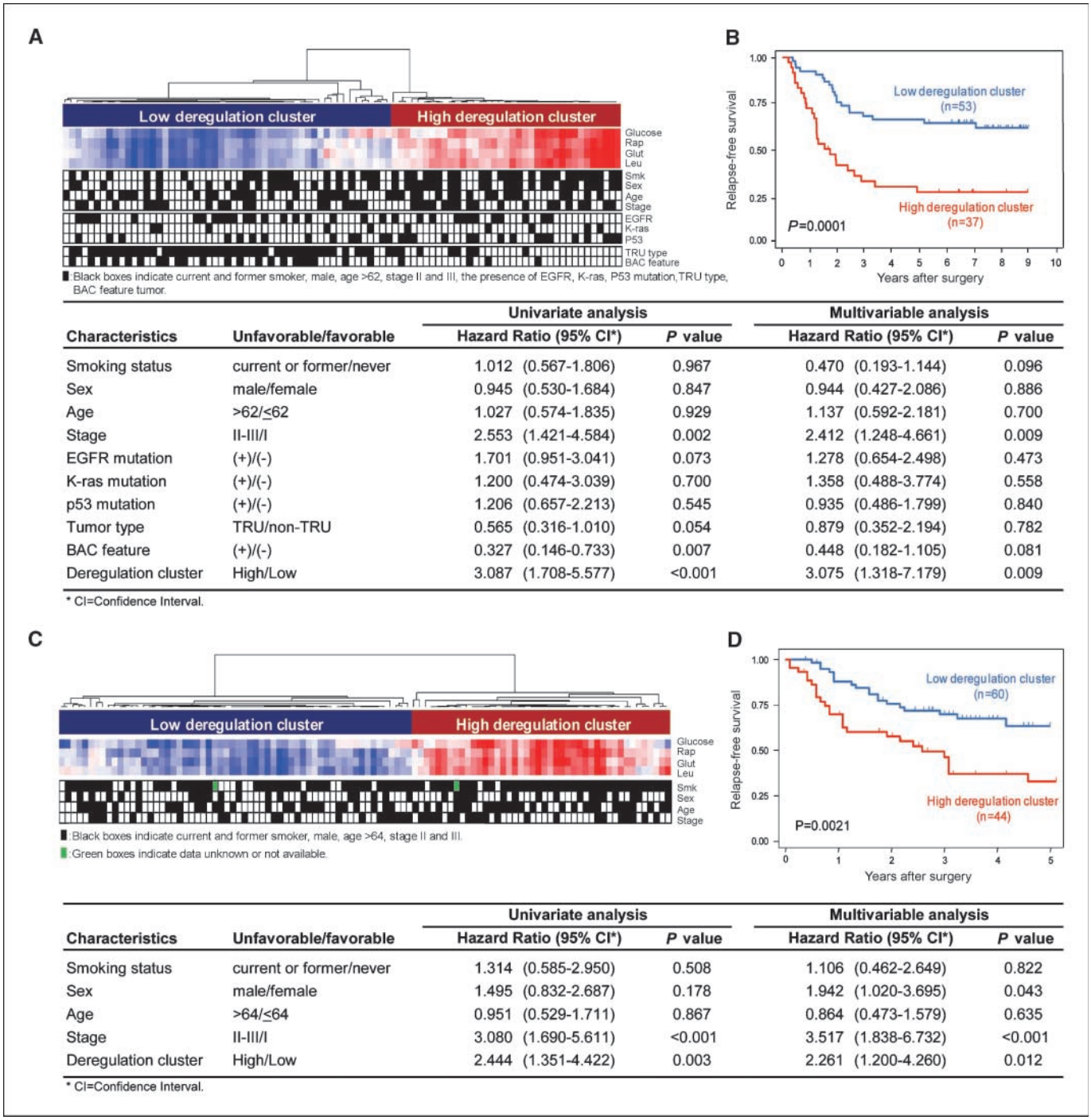

		Univariate analysis		Multivariable analysis	
Characteristics	Unfavorable/favorable	Hazard Ratio (95% CI*)	*P* value	Hazard Ratio (95% CI*)	*P* value
Smoking status	current or former/never	1.012 (0.567-1.806)	0.967	0.470 (0.193-1.144)	0.096
Sex	male/female	0.945 (0.530-1.684)	0.847	0.944 (0.427-2.086)	0.886
Age	>62/≤62	1.027 (0.574-1.835)	0.929	1.137 (0.592-2.181)	0.700
Stage	II-III/I	2.553 (1.421-4.584)	0.002	2.412 (1.248-4.661)	0.009
EGFR mutation	(+)/(-)	1.701 (0.951-3.041)	0.073	1.278 (0.654-2.498)	0.473
K-ras mutation	(+)/(-)	1.200 (0.474-3.039)	0.700	1.358 (0.488-3.774)	0.558
p53 mutation	(+)/(-)	1.206 (0.657-2.213)	0.545	0.935 (0.486-1.799)	0.840
Tumor type	TRU/non-TRU	0.565 (0.316-1.010)	0.054	0.879 (0.352-2.194)	0.782
BAC feature	(+)/(-)	0.327 (0.146-0.733)	0.007	0.448 (0.182-1.105)	0.081
Deregulation cluster	High/Low	3.087 (1.708-5.577)	<0.001	3.075 (1.318-7.179)	0.009

* CI=Confidence Interval.

		Univariate analysis		Multivariable analysis	
Characteristics	Unfavorable/favorable	Hazard Ratio (95% CI*)	*P* value	Hazard Ratio (95% CI*)	*P* value
Smoking status	current or former/never	1.314 (0.585-2.950)	0.508	1.106 (0.462-2.649)	0.822
Sex	male/female	1.495 (0.832-2.687)	0.178	1.942 (1.020-3.695)	0.043
Age	>64/≤64	0.951 (0.529-1.711)	0.867	0.864 (0.473-1.579)	0.635
Stage	II-III/I	3.080 (1.690-5.611)	<0.001	3.517 (1.838-6.732)	<0.001
Deregulation cluster	High/Low	2.444 (1.351-4.422)	0.003	2.261 (1.200-4.260)	0.012

* CI=Confidence Interval.

Figure 2. Relationships between deregulation of pathways converging onto mTOR and various features. *A, top,* hierarchical clustering of 90 adenocarcinoma samples from the Nagoya data set based on deregulation indices of metabolic gene sets. *Bottom,* relationships between two major branches and clinicopathologic and genetic characteristics. *B, top,* Kaplan-Meier survival curves according to the two major branches shown in *A* (*P* = 0.0001 by log-rank test). *Bottom,* results of univariate and multivariate Cox regression analyses. *C, top,* hierarchical clustering of 104 adenocarcinoma samples from the Memorial Sloan-Kettering Cancer Center data set based on deregulation indices of metabolic gene sets. *Bottom,* relationships between two major branches and clinicopathologic characteristics. Two cases lacked information regarding smoking history. *D, top,* Kaplan-Meier survival curves according to the two major branches shown in *C* (*P* = 0.0021 by log-rank test). *Bottom,* results of univariate and multivariate Cox regression analyses.

3-kinase (PI3K), as well as sirolimus (rapamycin), which inhibits mTOR, were ranked near the top of the C-MAP list of FDA-approved drugs (Supplementary Table S9 and Supplementary Fig. S3 showing results of the permutation test). In addition to the cancer-related kinase inhibitors, C-MAP analysis also identified several other unexpected agents with distant connections to cancer treatment, which included phenothiazine antipsychotics (prochlorperazine, trifluoperazine, fluphenazine, and thioridazine) and resveratrol, raising the possibility that these agents may also inhibit the same signaling pathways, exhibiting antitumor effects.

Finally, we analyzed whether changes in gene expression before and after rapamycin treatment in the ACC-LC-94 and A549 lung cancer cell lines corresponded to those in MCF-7, because the C-MAP database is mainly based on the expression profiling results in the MCF-7 breast cancer cell line. As a result, C-MAP analysis using the extracted probe sets exhibiting a significant response to rapamycin faithfully selected sirolimus (rapamycin) as significant (Supplementary Tables S10 and S11; $P = 0.0079$ in ACC-LC-94 and $P = 0.0105$ in A549 by permutation test).

Experimental validation of results obtained by the C-MAP analysis. To experimentally validate our results obtained by C-MAP analysis, we examined the growth inhibitory activities of the C-MAP–identified agents using a panel of lung cancer cell lines. Rapamycin and LY-294002 exhibited growth inhibitory activities in MTT assays, as expected, whereas prochlorperazine and resveratrol treatments also resulted in growth inhibition, athough rapamycin did not reach 50% growth inhibition with most of the lung cancer cell lines tested in this study (Supplementary Fig. S4). Notably, there was a significant inhibition of phosphorylation of p70 S6K, a downstream effecter of mTOR, in the A549 adenocarcinoma cell line by treatment with not only rapamycin and LY-294002 but also prochlorperazine and resveratrol. Inhibition of AKT phosphorylation was also detected in A549 cells treated with resveratrol or LY-294002, whereas prochlorperazine elicited a delayed induction of AKT similar to that observed with rapamycin (Fig. 3*C*). In addition, the expression of EGFR was down-regulated by treatment with prochlorperazine via a currently unknown mechanism (Supplementary Fig. S5). In addition to down-regulation of the prosurvival effectors, resveratrol induced marked phosphorylation of p38 MAP kinase, a proapoptotic effector, as well as modest phosphorylation of AMP kinase, which is activated by deprivation of cellular energy (13, 14), leading to inhibition of mTOR activity (Fig. 3*D*). These results showed that these compounds, which were identified *in silico*, as drugs with potential activities to alter a relapse-related death signature have effects on pathways converging onto mTOR with antitumor activities *in vitro*.

Requirement of inhibition of both mTORC1 and TORC2 for growth suppression of lung cancer cells. The modest growth inhibitory activity seen for the mTOR-inhibiting rapamycin led us to investigate the contribution of a delayed reactivation of AKT induced by rapamycin. Rapamycin treatment diminished the binding of mTOR with raptor, although a complex of mTOR and rictor (mTORC2) was still formed in the presence of rapamycin (Fig. 4*A*). siRNA-mediated knockdown of rictor caused a significant reduction in cell growth, which was enhanced by combined use with rapamycin (Fig. 4*B*). A reduction in the expression of rictor decreased the levels of phosphorylation of both AKT and FoxO3a, well-established direct substrates of AKT, whereas the phosphorylation of S6 kinase was marginally inhibited by knockdown of rictor (Fig. 4*C*), showing that simultaneous inhibition of mTORC1 and mTORC2 effectively inhibits cell growth in lung adenocarcinomas. In line with this observation, combined treatment of rapamycin with LY-294002 exhibited inhibition of rapamycin-mediated reactivation of AKT, in association with a more pronounced cell growth inhibition in lung cancer cell lines (Supplementary Fig. S6). We also found that concomitant treatment with resveratrol similarly inhibited reactivation of AKT in lung cancer cell lines treated with rapamycin (Fig. 4*D*).

Association of deregulation of GSEA-identified gene sets with sensitivity to the multikinase inhibitor PI-103. Our findings of effective growth inhibition of lung adenocarcinoma cells by combined inhibition of signaling involving PI3K, mTORC1, and mTORC2 led us to examine the inhibitory effects of PI-103, a small molecule with the capability to inhibit those three (Supplementary Fig. S7), in relation to the deregulation state of signaling converging onto mTOR (16, 17). Treatment with PI-103 clearly inhibited phosphorylation of AKT and S6K, as well as PDK1 downstream of PI3K in a dose-dependent manner in

Table 1. Results of connectivity map analysis (top 20 list of instances)

Rank	C-MAP name	Dose	Cell	Remarks
1	Wortmannin	1 μmol/L	MCF7	PI3K inhibitor
2	Resveratrol	10 μmol/L	MCF7	Polyphenolic compounds
3	Prochorperazine	10 μmol/L	MCF7	Phenothiazine antipsychotics
4	Trifluoperazine	10 μmol/L	MCF7	Phenothiazine antipsychotics
5	Resveratrol	10 μmol/L	MCF7	Polyphenolic compounds
6	Sirolimus	100 nmol/L	MCF7	mTOR inhibitor
7	Pyrvinium	1 μmol/L	MCF7	Antihelminthic
8	Trifluoperazine	10 μmol/L	MCF7	Phenothiazine antipsychotics
9	Sirolimus	100 nmol/L	MCF7	mTOR inhibitor
10	Sirolimus	100 nmol/L	MCF7	mTOR inhibitor
11	Rottlerin	10 μmol/L	MCF7	PKC inhibitor
12	Fluphenazine	10 μmol/L	MCF7	Phenothiazine antipsychotics
13	Calmidazolium	5 μmol/L	MCF7	Calmodulin inhibitor
14	Trichostatin A	100 nmol/L	MCF7	HDAC inhibitor
15	LY-294002	10 μmol/L	ssMCF7	PI3K inhibitor
16	Wortmannin	10 nmol/L	MCF7	PI3K inhibitor
17	Sirolimus	100 nmol/L	MCF7	mTOR inhibitor
18	Thioridazine	10 μmol/L	MCF7	Phenothiazine antipsychotics
19	LY-294002	10 μmol/L	MCF7	PI3K inhibitor
20	5248896	11 μmol/L	MCF7	Not assessed

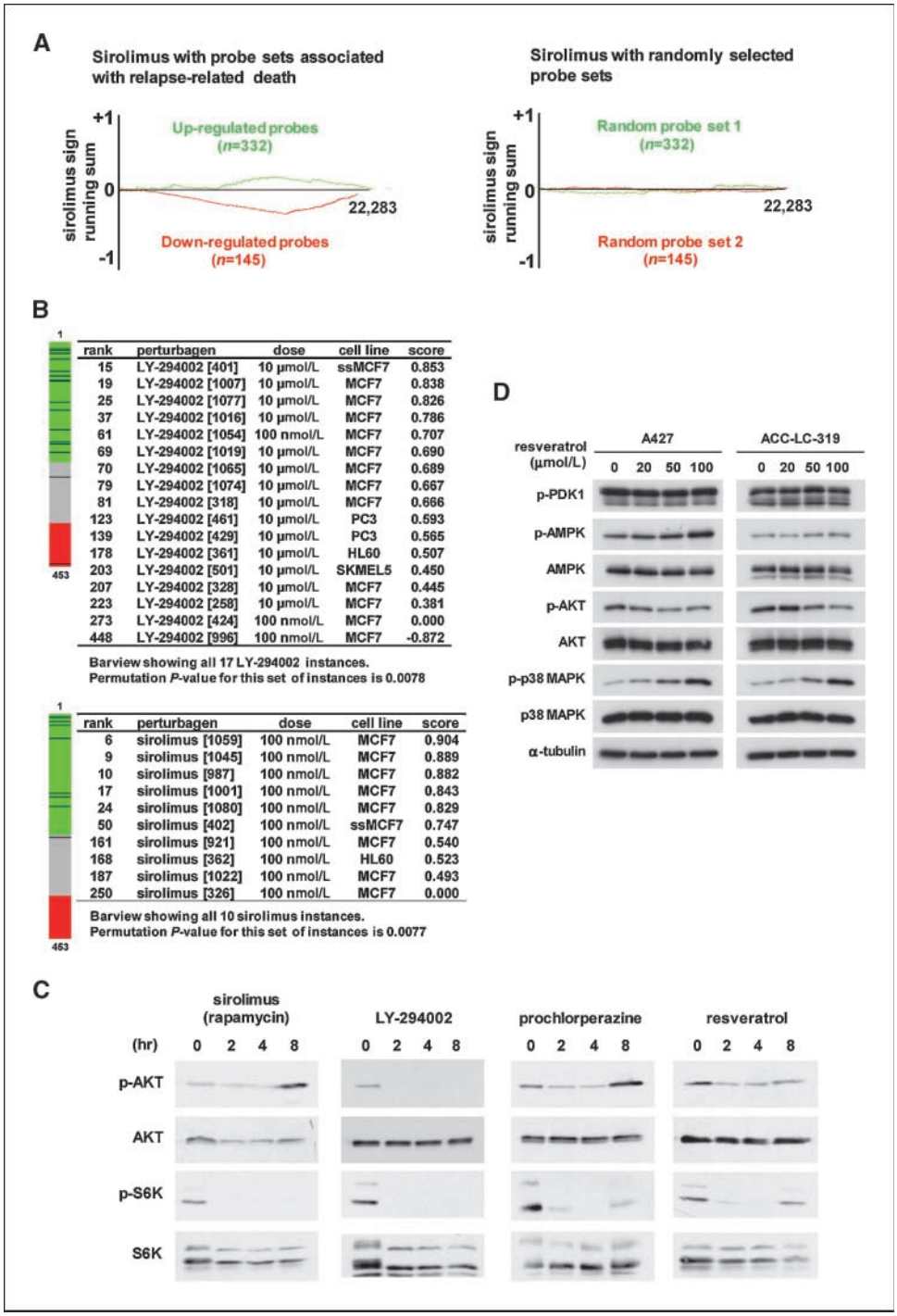

Figure 3. Identification of potential fatal prognosis–altering agents obtained using C-MAP analysis. *A,* representative results showing enrichment of outcome-associated probe sets for the sixth ranked sirolimus (*left*), which was not seen with the same numbers of randomly selected probe sets (*right*). Down-regulated (*green*) and up-regulated (*red*) gene probes associated with outcome were projected to the feature set based on the extent of differential expression in the instance of sirolimus (*x* axis, 22,283 probes). *B,* bar view showing high rankings for sirolimus and LY-294002. *C,* effects on signaling converging onto mTOR. *D,* effects of resveratrol treatment on prosurvival and proapoptotic effectors, as well as AMP kinase (*AMPK*). Cells were treated for 6 h with the indicated agents.

A549 and ACC-LC-319 cells (Fig. 5*A*). The level required for 50% growth inhibition in the panel of 11 lung adenocarcinoma cell lines ranged from 0.2 to 2.7 µmol/L (Supplementary Table S12). Intriguingly, the cumulative deregulation score, which we defined on the basis of the cumulative deregulation of each gene set, including Rap_down, Glucose_down, Leu_down, and Glut_down, was found to be associated with sensitivities to PI-103 in each lung adenocarcinoma cell line (Fig. 5*B*; $r = 0.667$, $P = 0.025$ by Pearson's correlation coefficient), suggesting the potential usefulness of such a cumulative deregulation score for predicting the sensitivity to PI-103 and possibly of other agents simultaneously affecting multiple molecules in pathways converging onto mTOR.

Discussion

Rapid proliferation of cancer cells causes an insufficient blood supply, which elicits a variety of environmental stresses, such as deprivation of growth factors, nutrients, and/or oxygen. However, cancer cells are thought to be capable of surviving in spite of such

constraints, which conceivably leads to disease progression and ultimately confers poor prognosis in affected patients. A number of studies have aimed at identifying a list of genes related to lung cancer prognosis (2, 3, 10, 18–21); however, criticism is frequently raised noting that the gene lists used in such prognosis prediction classifiers have minimal overlaps and provide little biological insight into the underlying mechanisms. In a related study, Bild and colleagues analyzed artificially generated cells with overexpression of various oncogenes *in vitro* and identified oncogenic pathway signatures with a potential to separate lung cancer patients into subgroups in relation to outcome, including drug sensitivity (22). In contrast, the present study, which used two independent bioinformatics approaches, namely GSEA and C-MAP analysis, directly used expression profiles of patient tumors. We specifically designed our study to focus on the underlying molecular basis linking poor prognosis with particular pathways and/or functions of the gene sets involved, which showed the association of deregulation of multiple signaling converging onto mTOR with relapse and death in lung adenocarcinoma patients.

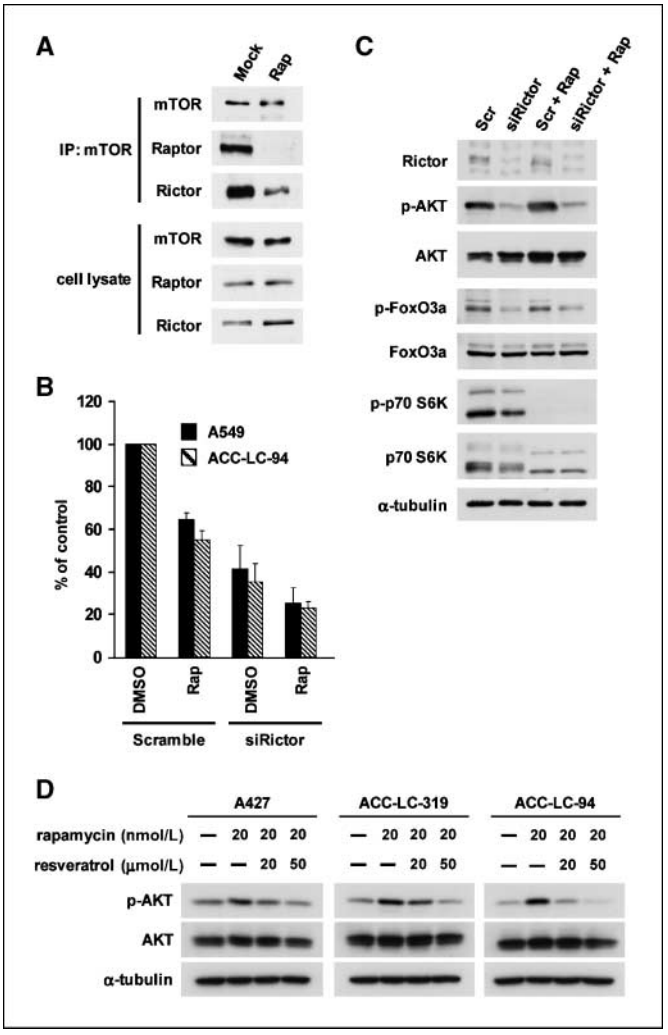

Figure 4. Enhanced inhibition by concurrent blocking of PI3K and mTORC1 or both mTOR complexes. *A,* immunoprecipitation analysis of A549 cells treated with rapamycin. *B* and *C,* effects of rictor knockdown on cell growth (*B*) and signaling converging onto mTOR (*C*). *Columns,* mean from four experiments; *bars,* SD. *D,* Western blot analysis showing resveratrol-mediated reduction of rapamycin-induced up-regulation of AKT. Cells were treated for 6 h with the indicated agents.

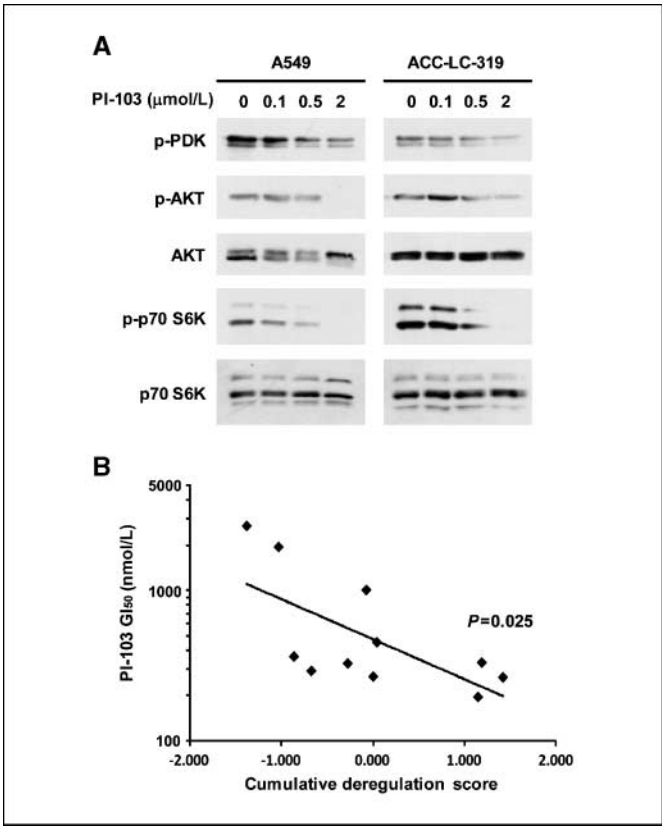

Figure 5. Relationships of deregulation of identified gene sets with sensitivities to PI-103. *A,* Western blot analysis of A549 and ACC-LC-319 cells treated with PI-103 for 4 h. *B,* scattered plot analysis showing an increased probability of sensitivity to PI-103 in cell lines with more pronounced deregulation ($r = 0.667$, $P = 0.025$).

Activation of the PI3K-AKT-mTOR axis plays a key role in growth factor receptor–mediated signaling for cancer cell growth and survival, whereas LKB1, which is inactivated in a fraction of lung adenocarcinomas (23, 24), activates AMP kinase in microenvironmental conditions, including insufficient nutrients, and leads to inhibition of mTOR activity in an AKT-independent manner (13, 14). In addition, amino acids, such as leucine, regulate mTOR signaling, which involves raptor, a ras homologue enriched in the brain, and a GTPase that activates mTOR, which are directly associated with mTOR (25, 26). This study is the first to report that the expression state of genes affected by withdrawal of amino acids is significantly altered in association with poor prognosis, suggesting that adaptation to an insufficient availability of amino acids may be a prerequisite for the progression of lung adenocarcinomas. In addition, the expression state of genes responsive to glucose withdrawal was found to be altered in tumors associated with a fatal outcome at a more pronounced level, a finding consistent with a previous report by Chen and colleagues that found increased expression of glycolytic enzymes in association with poor prognosis (27). In our multivariate Cox regression analysis, deregulation of mTOR-converging signaling seemed to be an independent prognostic factor in addition to disease stage, whereas such statistical significance was not observed with various other parameters,

including mutations of *EGFR, K-ras*, and *p53*, as well as bronchioloalveolar carcinoma features and TRU/non-TRU classification. Multivariate Cox regression analysis of the Memorial Sloan-Kettering Cancer Center data sets also showed similar associations, supporting the notion that deregulation of mTOR-converging signaling may be a generic signature in patients with a high risk for relapse and fatal outcome. It is interesting that two independent groups recently reported a lack of prognostic value of *LKB1* inactivation in lung cancers (28, 29), whereas conflicting results were presented in terms of the association between poor prognosis and AKT phosphorylation (30–32). Therefore, it is possible that an altered state of multiple signaling converging onto mTOR may be more reflected in clinical behavior rather than a given molecule in the pathways.

Also interesting is that our *in silico* search using C-MAP analysis for drugs with activities that potentially revert a fatal prognosis-associated signature to a favorable prognosis-associated one resulted in identification of not only well-known inhibitors of PI3K or mTOR, but also several unexpected ones, such as those with antitumor activities *in vitro*. It has been reported that whereas rapamycin and its derivatives exhibit considerable antitumor activity in certain tumor types, including renal cell carcinoma, mantle cell lymphoma, and endometrial cancers, lung cancers are rather resistant with response rates of <10% (33). In this connection, the present results obtained with siRNA-mediated silencing of rictor in the presence of rapamycin suggest that enhanced effectiveness may be attained by concomitant inhibition of mTORC1 and mTORC2. We also unexpectedly identified drugs, including phenothiazine antipsychotics (prochlorperazine, trifluoperazine, fluphenazine, and thioridazine), an antihelminthic (pyrvinium), and resveratrol, a chemopreventive agent (34). In addition, prochlorperazine was shown here for the first time to inhibit mTOR-mediated signaling and induce a delayed phosphorylation of AKT in a manner similar to rapamycin. It is also important to note that both rapamycin and prochlorperazine have abilities to promote autophagy (35), a cellular response to a growth factor/nutrient–deprived condition. Pyrvinium was previously shown to inhibit cancer cell survival by blocking AKT signaling specifically in a nutrient-starved condition, which is also consistent with the present findings (36). Interestingly, whereas this study showed that PI-103, a dual specificity kinase inhibitor, inhibited growth of lung adenocarcinoma cell lines through concurrent inhibition of PI3K and mTOR without AKT feedback activation, we observed an inverse relationship between cumulative deregulation score, i.e., extent of augmentation in the expression signatures of gene sets related to mTOR-converging signaling, and sensitivity to PI-103, providing further support to a functionally relevant connection.

In conclusion, using two independent bioinformatics approaches, we identified a significant association between deregulation of signaling converging onto mTOR and poor prognosis in lung adenocarcinomas, suggesting the existence of gene set–definable, intrinsic heterogeneities in this devastating tumor type. In addition, our results lend support to the notion that compounds identified by *in silico* screening as having potential activities to alter signatures associated with relapse and death to favorable ones can be anticipated to show antitumor activities and inhibitory effects on pathways converging onto mTOR.

Disclosure of Potential Conflicts of Interest

No potential conflicts of interest were disclosed.

Acknowledgments

Received 9/2/08; revised 1/19/09; accepted 2/24/09; published OnlineFirst 4/21/09.

Grant support: Ministry of Education, Culture, Sports, Science and Technology of Japan grant-in-aid for Scientific Research on Priority Areas (T. Takahashi) and Japan Society for the Promotion of Science grant-in-aid for Young Scientists (B) (S. Tomida). H. Ebi was supported by the International Association for the Study of Lung Cancer fellowship during the study.

The costs of publication of this article were defrayed in part by the payment of page charges. This article must therefore be hereby marked *advertisement* in accordance with 18 U.S.C. Section 1734 solely to indicate this fact.

References

1. Takeuchi T, Tomida S, Yatabe Y, et al. Expression profile-defined classification of lung adenocarcinoma shows close relationship with underlying major genetic changes and clinicopathologic behaviors. J Clin Oncol 2006;24:1679–88.
2. Beer DG, Kardia SL, Huang CC, et al. Gene-expression profiles predict survival of patients with lung adenocarcinoma. Nat Med 2002;8:816–24.
3. Potti A, Mukherjee S, Petersen R, et al. A genomic strategy to refine prognosis in early-stage non-small-cell lung cancer. N Engl J Med 2006;355:570–80.
4. Tomida S, Koshikawa K, Yatabe Y, et al. Gene expression-based, individualized outcome prediction for surgically treated lung cancer patients. Oncogene 2004;23:5360–70.
5. Lau SK, Boutros PC, Pintilie M, et al. Three-gene prognostic classifier for early-stage non small-cell lung cancer. J Clin Oncol 2007;25:5562–9.
6. Tomida S, Takeuchi T, Shimada Y, et al. Relapse-related molecular signature in lung adenocarcinoma identifies patients with dismal prognosis. J Clin Oncol. In press 2009, doi:10.1200/JCO.2008.19.7053.
7. Subramanian A, Tamayo P, Mootha VK, et al. Gene set enrichment analysis: a knowledge-based approach for interpreting genome-wide expression profiles. Proc Natl Acad Sci U S A 2005;102:15545–50.
8. Lamb J, Crawford ED, Peck D, et al. The Connectivity Map: using gene-expression signatures to connect small molecules, genes, and disease. Science 2006;313:1929–35.
9. Ramaswamy S, Ross KN, Lander ES, Golub TR. A molecular signature of metastasis in primary solid tumors. Nat Genet 2003;33:49–54.
10. Shedden K, Taylor JM, Enkemann SA, et al. Gene expression-based survival prediction in lung adenocarcinoma: a multi-site, blinded validation study. Nat Med 2008;14:822–7.
11. Eisen MB, Spellman PT, Brown PO, Botstein D. Cluster analysis and display of genome-wide expression patterns. Proc Natl Acad Sci U S A 1998;95:14863–8.
12. Schmelzle T, Hall MN. TOR, a central controller of cell growth. Cell 2000;103:253–62.
13. Inoki K, Corradetti MN, Guan KL. Dysregulation of the TSC-mTOR pathway in human disease. Nat Genet 2005;37:19–24.
14. Guertin DA, Sabatini DM. Defining the role of mTOR in cancer. Cancer Cell 2007;12:9–22.
15. Wei G, Twomey D, Lamb J, et al. Gene expression-based chemical genomics identifies rapamycin as a modulator of MCL1 and glucocorticoid resistance. Cancer Cell 2006;10:331–42.
16. Knight ZA, Gonzalez B, Feldman ME, et al. A pharmacological map of the PI3-K family defines a role for p110α in insulin signaling. Cell 2006;125:733–47.
17. Fan QW, Knight ZA, Goldenberg DD, et al. A dual PI3 kinase/mTOR inhibitor reveals emergent efficacy in glioma. Cancer Cell 2006;9:341–9.
18. Lu Y, Lemon W, Liu PY, et al. A gene expression signature predicts survival of patients with stage I non-small cell lung cancer. PLoS Med 2006;3:e467.
19. Chen HY, Yu SL, Chen CH, et al. A five-gene signature and clinical outcome in non-small-cell lung cancer. N Engl J Med 2007;356:11–20.
20. Bianchi F, Nuciforo P, Vecchi M, et al. Survival prediction of stage I lung adenocarcinomas by expression of 10 genes. J Clin Invest 2007;117:3436–44.
21. Larsen JE, Pavey SJ, Passmore LH, Bowman RV, Hayward NK, Fong KM. Gene expression signature predicts recurrence in lung adenocarcinoma. Clin Cancer Res 2007;13:2946–54.
22. Bild AH, Yao G, Chang JT, et al. Oncogenic pathway signatures in human cancers as a guide to targeted therapies. Nature 2006;439:353–7.
23. Ji H, Ramsey MR, Hayes DN, et al. LKB1 modulates lung cancer differentiation and metastasis. Nature 2007;448:807–10.
24. Shah U, Sharpless NE, Hayes DN. LKB1 and lung cancer: more than the usual suspects. Cancer Res 2008;68:3562–5.

25. Roos S, Jansson N, Palmberg I, Saljo K, Powell TL, Jansson T. Mammalian target of rapamycin in the human placenta regulates leucine transport and is down-regulated in restricted fetal growth. J Physiol 2007; 582:449–59.
26. Kimball SR, Jefferson LS. Signaling pathways and molecular mechanisms through which branched-chain amino acids mediate translational control of protein synthesis. J Nutr 2006;136:227–31S.
27. Chen G, Gharib TG, Wang H, et al. Protein profiles associated with survival in lung adenocarcinoma. Proc Natl Acad Sci U S A 2003;100:13537–42.
28. Conde E, Suarez-Gauthier A, Garcia-Garcia E, et al. Specific pattern of LKB1 and phospho-acetyl-CoA carboxylase protein immunostaining in human normal tissues and lung carcinomas. Hum Pathol 2007;38:1351–60.
29. Onozato R, Kosaka T, Achiwa H, et al. LKB1 gene mutations in Japanese lung cancer patients. Cancer Sci 2007;98:1747–51.
30. Balsara BR, Pei J, Mitsuuchi Y, et al. Frequent activation of AKT in non-small cell lung carcinomas and preneoplastic bronchial lesions. Carcinogenesis 2004;25:2053–9.
31. Massion PP, Taflan PM, Shyr Y, et al. Early involvement of the phosphatidylinositol 3-kinase/Akt pathway in lung cancer progression. Am J Respir Crit Care Med 2004;170:1088–94.
32. Tsurutani J, Fukuoka J, Tsurutani H, et al. Evaluation of two phosphorylation sites improves the prognostic significance of Akt activation in non-small-cell lung cancer tumors. J Clin Oncol 2006;24: 306–14.
33. Gridelli C, Maione P, Rossi A. The potential role of mTOR inhibitors in non-small cell lung cancer. Oncologist 2008;13:139–47.
34. Baur JA, Sinclair DA. Therapeutic potential of resveratrol: the *in vivo* evidence. Nat Rev Drug Discov 2006;5:493–506.
35. Zhang L, Yu J, Pan H, et al. Small molecule regulators of autophagy identified by an image-based high-throughput screen. Proc Natl Acad Sci U S A 2007;104: 19023–8.
36. Esumi H, Lu J, Kurashima Y, Hanaoka T. Antitumor activity of pyrvinium pamoate, 6-(dimethylamino)-2-[2-(2,5-dimethyl-1-phenyl-1H-pyrrol-3-yl)ethenyl]-1-methyl-quinolinium pamoate salt, showing preferential cytotoxicity during glucose starvation. Cancer Sci 2004; 95:685–90.